

DMD # 18242

Taxane's substituents at C3' affect its regioselective metabolism

Different in vitro metabolism of cephalomannine and paclitaxel

Jiang-Wei Zhang, Guang-Bo Ge, Yong Liu, Li-Ming Wang, Xing-Bao Liu, Yan-Yan

Zhang, Wei Li, Yu-Qi He, Zheng-Tao Wang, Jie Sun, Hong-Bin Xiao, Ling Yang

Laboratory of Pharmaceutical Resource Discovery (J.W.Z., G.B.G., Y.L., X.B.L., Y.Y.Z., W.L., L.Y.), and Laboratory of Medical Chemistry (H.B.X.), Dalian Institute of Chemical Physics, Chinese Academy of Sciences, Dalian, China; The Second Affiliated Hospital of Dalian Medical University, Dalian, China (L.M.W., J.S.); Shanghai University of Traditional Chinese Medicine, Shanghai, China (Y.Q.H., Z.T.W.); Graduate School of Chinese Academy of Sciences, Beijing, China (J.W.Z., G.B.G., Y.Y.Z., W.L.)

DMD # 18242

Running title: Different metabolism of cephalomannine and paclitaxel

Author for correspondence: Dr. & Prof. Ling Yang, Laboratory of Pharmaceutical Resource Discovery, Dalian Institute of Chemical Physics, Chinese Academy of Sciences, Dalian, 116023 China, Tel: +86-411-84379317, Fax: +86-411-84676961, E-mail: yling@dicp.ac.cn

Number of Text Pages: 42

Number of Tables: 5

Number of Figures: 8

Number of References: 40

Number of Words

In the Abstract: 232

In the Introduction: 549

In Discussion: 1073

Abbreviations:

HLMs, human liver microsomes; RLMS, rat liver microsomes; PLMs, minipig liver microsomes; CYP, cytochrome P450; DH, bond dissociation energy

DMD # 18242

Abstract

To investigate how taxane's substituents at C3' affect its metabolism, we compared the metabolism of cephalomannine and paclitaxel, a pair of analogue which differ slightly at C3' position. After cephalomannine was incubated with human liver microsomes in a NADPH-generating system, two mono-hydroxylated metabolites (M-1, M-2) were detected by LC/MS/MS. C4" (M-1) and C6 α (M-2) were proposed as the possible hydroxylation sites, and the structure of M-1 was confirmed by ¹HNMR. Chemical inhibition studies and assays with recombinant human CYPs indicated that 4"-hydroxycephalomannine was generated predominantly by CYP3A4 and 6 α -hydroxycephalomannine by CYP2C8. The overall biotransformation rate between paclitaxel and cephalomannine differed slightly (184 *versus* 145 pmol/min/mg), but the average ratio of metabolites hydroxylated at C13 side chain to C6 α for paclitaxel and cephalomannine varied significantly (15:85 *versus* 64:36) in five human liver samples. Compared with paclitaxel, the major hydroxylation site transferred from C6 α to C4", and the main metabolizing CYP changed from CYP2C8 to CYP3A4 for cephalomannine. In the incubation system with rat or minipig liver microsomes, only 4"-hydroxycephalomannine was detected, and its formation was inhibited by CYP3A inhibitors. Molecular docking by Autodock suggested that cephalomannine adopted an orientation in favor of 4"-hydroxylation, while paclitaxel adopted an orientation favoring 3'-p-hydroxylation. Kinetic studies showed that CYP3A4 catalyzed cephalomannine more efficiently than paclitaxel due to an increased V_m. Our results demonstrate that relative minor modification of taxane at C3' have major consequence on

DMD # 18242

the metabolism.

Introduction

Paclitaxel is one of the best antineoplastic drugs derived from the yew trees, and it has been found effective against a broad spectrum of cancers (Spratlin and Sawyer, 2007). The superior anti-tumor activity of paclitaxel, however, is undermined by limitations such as multi-drug resistance, poor aqueous solubility, poor oral bioavailability, and toxicities (Frapolli et al., 2006). It's generally recognized that poor oral bioavailability of paclitaxel results from its poor solubility (Singla et al., 2002) and Pgp efflux (Sparreboom et al., 1997). To overcome these shortcomings, numerous novel taxanes superior to paclitaxel were synthesized (Ojima et al., 1996; Mastalerz et al., 2003; Barboni et al., 2005; Lockhart et al., 2007), and some of them such as BAY59-8862 (Sano et al., 2006), BMS-275183 (Broker et al., 2007), and MAC-321 (Lockhart et al., 2007) entered clinical trials. Many of these novel taxanes had modified substituents at C3' of the C13 side chain, where two phenyls were replaced by other functional groups (Sano et al., 2006; Broker et al., 2007; Lockhart et al., 2007). These structure modifications made the novel taxanes effective to paclitaxel-resistant tumor cells, more soluble, and/or more potent. It's still not clear how these structure changes at C3' affect taxane's metabolism property, which is crucial to efficacy, toxicity, route of administration, pharmacokinetics, and pharmacodynamics (Taniguchi et al., 2005; Spratlin and Sawyer, 2007).

CYP-mediated oxidative metabolism is the major elimination routine for taxanes (Anderson et al., 1995; Cresteil et al., 2002), which differ strikingly from one another in metabolism despite structure similarity. For example, when benzamide at C3' in

DMD # 18242

paclitaxel was replaced by boc-amino group in docetaxel, the principal hydroxylation site transferred from C6 of the taxane ring to the tert-butyl of the side chain (Cresteil et al., 2002; Taniguchi et al., 2005). Meanwhile, the primary monooxygenases changed from CYP2C8 to CYP3A4 (Cresteil et al., 2002; Taniguchi et al., 2005). Interestingly, when both phenyls at C3' of C13 side chain were replaced by alkyl or alkenyl group, the major hydroxylation site was again moved from tert-butyl back to the isobutyl or isobutenyl group, such as SB-T-1102, SB-T-1214, SB-T-1216 (Gut et al., 2006), and IDN5390 (Frapolli et al., 2006). All these results suggested that substituents at C3' determined taxane metabolism with regard to the site of hydroxylation and the CYP isoform implicated.

Cephalomannine (also known as taxol B) is an analogue of paclitaxel commonly occurring in yew extracts (Mroczek et al., 2000). It differs from paclitaxel only in the amide portion; the substituent at C3' position is tigloylamide instead of benzamide (Fig. 1). Due to structure similarity, cephalomannine shows anti-tumor activity comparable to paclitaxel towards several different cell lines (Helson and Ainsworth, 1997; Shi et al., 2001). It is especially effective against leukemia and certain neural tumor cells (Helson and Ainsworth, 1997). Despite its promising anti-tumor activity, relatively little is known about the metabolism of cephalomannine.

In the present study, we chose cephalomannine, an analogue of paclitaxel with slight modification at C3', to study the effect of structure change on metabolism. LC/MS/MS and ¹HNMR were recruited to identify the structures of the observed metabolites. Incubations were conducted with CYP isoform specific inhibitors and re-

DMD # 18242

combinant human CYP isoforms to ascribe individual biotransformation to a single CYP isoform. To compare species difference, metabolism of cephalomannine in rat and minipig liver microsomes were also examined.

Materials and Methods

Chemicals. D-glucose-6-phosphate, glucose-6-phosphate dehydrogenase, NADP⁺, sulfaphenazole, quinidine, clomethiazole, furafylline, 8-methoxypsoralen, 3'-p-hydroxypaclitaxel, and paclitaxel were purchased from Sigma-Aldrich (St. Louis, MO, USA). Ketoconazole was obtained from ICN Biomedicals Inc. (Aurora, Ohio, USA). S-mephenytoin was purchased from Toronto Research Chemicals Inc. (North York, Canada). 6 α -hydroxypaclitaxel was obtained from BD Gentest Corp. (Woburn, MA, USA). Quercetin was purchased from Acros Organics (Geel, Belgium). Cephalomannine (96%) was purchased from Shanghai Jinhe Bio-Technology Co. (Shanghai, China). All other reagents were of HPLC grade or of the highest grade commercially available. cDNA-expressed recombinant CYP1A2, CYP2A6, CYP2C9, CYP2D6, CYP2E1 and CYP3A4 derived from baculovirus infected insect cells coexpressing NADPH-P450 reductase was obtained from BD Gentest Corp. (Woburn, MA, USA). cDNA-expressed CYP2C8 and CYP2C19 in *Escherichia coli* coexpressing NADPH-P450 reductase were purchased from New England Biolabs (Beijing) Ltd (Beijing, China).

Preparation and characterization of liver microsomes. Human livers were obtained from autopsy samples (n=5, male Chinese, ages from 27 to 48) from Dalian Medical University, with the approval of the ethics committee of Dalian Medical University. The medication history of the donors was not known. Research involving human subjects was done under full compliance with government policies and the Helsinki Declaration.

DMD # 18242

Procedures involving animals complied with the Laboratory Animal Management Principles of China. Sprague-Dawley (SD) rats (n=10, male, weight 180-220 g) were purchased from Dalian Medical University. The animals had free access to tap water and pellet diet. CYP was induced by phenobarbital (80 mg/kg, i.p.) in 24-h intervals for three days. The rats were euthanized by decapitation, and livers were rapidly excised and pooled for preparation of microsomes.

Colony-bred Chinese Bama minipig weighing 10 to 12 kg (n=6, male, age 6 months) were obtained from Department of Animal Science, 3rd Military Medical University, China. The animals used are descendants of sows and boars obtained from the original stock at Bama County, GuangXi Province, China. The animals were euthanized by intravenous injection of pentobarbital sodium (150 mg/kg body weight); tissue samples were taken from the left medial lobe of the liver within 5 min after death. Liver samples were pooled together to prepare microsomes.

Liver specimens were stored in liquid nitrogen until preparation of microsomes. Microsomes were prepared from liver tissue by differential ultracentrifugation as described previously (Li et al., 2006). Protein concentration was determined by using bovine serum albumin as standards (Lowry et al., 1951). Total CYP concentration was determined according to Omura and Sato (Omura and Sato, 1964) with the use of molar extinction coefficient $91 \text{ mM}^{-1}\cdot\text{cm}^{-1}$. Liver microsomes were diluted to 10 mg/mL and were stored at -80°C . CYP concentration was 0.63, 0.52, and 0.23-0.39 nmol/mg in minipig, rat, and human liver microsomes, respectively.

Incubation system. The incubation mixture, with a total volume of 200 μL , consisted of 100 mM potassium phosphate buffer (pH 7.4), NADPH-generating system (1 mM NADP^+ , 10 mM glucose-6-phosphate, 1 unit/mL of glucose-6-phosphate dehy-

DMD # 18242

drogenase, and 4 mM MgCl₂), liver microsomes (0.5 mg/mL), and 10 μM cephalomannine or paclitaxel. Taxanes were previously dissolved in methanol, with a final methanol concentration below 1% (v/v) in the reaction mixture. After 3-min preincubation at 37°C, the reaction was initiated by adding NADPH-generating system. After incubated for 30 min in a shaking water bath, the reaction was terminated by the addition of methanol (100 μL). The mixture was kept on ice until it was centrifuged at 20,000× *g* for 10 min at 4 °C. Aliquots of supernatants were transferred for HPLC analysis. Control incubations without NADPH or without substrate or without microsomes were carried out to ensure that metabolites formation were microsomes and NADPH dependent. The metabolites of cephalomannine were quantified based on the calibration curves of cephalomannine, assuming similar molar extinction coefficients. The metabolites of paclitaxel were quantified by comparing the calibration curves of 6α-hydroxypaclitaxel and 3'-p-hydroxypaclitaxel.

HPLC/MS method. The HPLC system (SHIMADZU, Kyoto, Japan) consisted of a SCL-10A system controller, two LC-10AT pumps, a SIL-10A auto injector, a SPD-10A_{VP} UV detector and a Shim-pack (Shimadzu corporation) C₁₈ column (4.6×150 mm, 5 μ) was used to separate taxanes and its metabolites. The mobile phase was 65% methanol in water. The eluent was monitored at 230 nm with a flow rate of 1.0 mL/min.

LC/MS was used to characterize the structures of cephalomannine metabolites. The HPLC eluent from detector was introduced into the mass spectrometer via a 1:4 split. The mass spectrometer was a TSQ triple quadrupole (Thermo Fisher Scientific,

DMD # 18242

Waltham, MA, USA) equipped with an ESI interface. The spray voltage was 4.5 kV and the capillary temperature was 300 °C. Nitrogen was used as nebulizing and auxiliary gas. The nebulizing gas backpressure was set at 40 psi, and auxiliary gas at 20 (arbitrary units). For MS/MS, argon at a pressure of 3 mTorr was used as the collision gas. The collision energy was set at 15-30 V. Initially, the mass spectrometer was programmed to perform full scans between m/z 200 and 1000 in order to observe the $[M+H]^+$ and $[M-H]^-$ signals.

Metabolite purification. Rat liver microsomes (RLMs) catalyze cephalomannine efficiently to one of its metabolites (M-1), this allowed for the preparation of sufficient quantities of M-1 for ^1H NMR analysis. The incubation system was scaled up to 250 mL. Cephalomannine (50 μM) was incubated with RLMs (1.0 mg/mL) and NADPH-generating system (1 mM NADP^+ , 10 mM glucose-6-phosphate, 1 unit/mL of glucose-6-phosphate dehydrogenase, and 4 mM MgCl_2) for 90 min at 37 °C. Under these conditions, about 20% of cephalomannine was converted to M-1. The reaction mixture was extracted with 50% ethyl acetate, and the organic layer was separated after the reaction mixture was centrifuged at $9000\times g$ for 10 min. The extraction procedure was repeated three times and the organic layer was combined. The organic phase was dried in vacuo, and the residue was dissolved in methanol (1.5 mL). Cephalomannine and its metabolite were separated by HPLC, and the eluent containing the metabolite was collected and dried in vacuo. The purity of M-1 was about 92% (HPLC).

NMR spectroscopy. Proton NMR spectra were obtained at 400 MHz on a Bruker

DMD # 18242

AV-400 spectrometer (Bruker, Newark, Germany). Compounds were dissolved in CDCl_3 and experiments were conducted at 21 °C. Chemical shifts are reported in ppm with reference to tetramethylsilane.

Chemical inhibition studies. Chemical inhibition studies were performed by adding different human CYP inhibitors to the incubation mixture of cephalomannine (20 μM) before the addition of NADPH-generating system. Information concerning the plasma concentration of cephalomannine was lacking. Selection of a 20 μM concentration was based on the plasma concentration of paclitaxel (C_{max} , 14 μM) (Bhalla et al., 1999). The selective inhibitors (or substrates) of eight major CYPs and their concentrations were as follows (Bjornsson et al., 2003; Huang et al., 2007): furafylline (10 μM) for CYP1A2, 8-methoxypsoralen (2.5 μM) for CYP2A6, quercetin (20 μM) for CYP2C8 (Harris et al., 1994), sulfaphenazole (10 μM) for CYP2C9, S-mephenytoin (100 μM) for CYP2C19, quinidine (10 μM) for CYP2D6, clomethiazole (50 μM) for CYP2E1, ketoconazole (1 μM) for CYP3A4. 8-methoxypsoralen is known as a mechanism-based inhibitor, so it was preincubated with human liver microsomes (HLMs), buffer, and NADPH-generating system at 37 °C for 10 min, and the reaction was initiated by the addition of cephalomannine.

Troleandomycin (Anzenbacher et al., 1998), ketoconazole (Li et al., 2006), sulfaphenazole (Kobayashi et al., 2003), and furafylline (Kobayashi et al., 2003) were found to be inhibitors of rat or minipig CYP3A, CYP2C and CYP1A, respectively. Therefore, inhibitory effects of troleandomycin (25 μM), ketoconazole (1 μM), sulfaphenazole (10 μM), and furafylline (10 μM) towards cephalomannine (10 μM) me-

DMD # 18242

tabolism in RLMs and minipig liver microsomes (PLMs) were examined. Troleanomycin was preincubated with liver microsomes, buffer, and NADPH-generating system at 37 °C for 10 min, and the reaction was initiated by the addition of cephalomannine.

Assay with recombinant human CYPs. cDNA-expressed recombinant human CYP isoforms co-expressing NADPH-P450 reductase either from insect cells (CYP1A2, CYP2A6, CYP2C9, CYP2D6, CYP2E1 and CYP3A4) or from *Escherichia coli* (CYP2C8 and CYP2C19) was used. The incubations were carried out as described for the human liver microsomal study. To examine the contribution of each CYP isoform, cephalomannine (60 μ M) was incubated with each of the recombinant CYPs (40-80 pmol of CYP/mL) at 37°C for 60 min. HPLC with UV detection was used to monitor possible metabolites. Relative high substrate concentration was selected so that adequate metabolites were generated for the convenience of detection.

Kinetic Assays. To estimate kinetic parameters, cephalomannine (4.0-70 μ M) or paclitaxel (2.0-50 μ M) was incubated with liver microsomes (0.5 mg/mL) or recombinant CYPs (40 nM) for 30 min. For RLMs, the incubation time was reduced to 10 min because of extensive metabolism of cephalomannine. The apparent V_m and K_m values were calculated from nonlinear regression analysis of experimental data according to the Michaelis-Menten equation, and the results were graphically represented by double-reciprocal plots of velocities versus concentrations of substrate. The H1 human liver microsomal sample was used in kinetics and inhibition studies because it exhibited high activity of CYP3A4 and CYP2C8, and enabled analysis of

DMD # 18242

both metabolites at low substrate concentrations. Preliminary experiments were carried out to make sure that formation of metabolites was in the linear range of both reaction time and the concentration of liver microsomes. All incubations were carried out in duplicate with SD values generally below 10%.

Molecular Docking. Autodock 4.0 (Scripps Research Institute, La Jolla, CA) (Morris et al., 1998) was used to dock paclitaxel and cephalomannine to the active site CYP3A4(PDB entry 2j0d) (Ekroos and Sjogren, 2006). The cocrystallized ligand erythromycin was removed from the protein structure before docking. 3D structures of paclitaxel and cephalomannine were obtained from National Cancer Institute database of small molecules (<http://129.43.27.140/ncidb2/>). AutoDockTools 1.4.5 (Scripps Research Institute, La Jolla, CA) (Sanner, 1999) was used to prepare all docking parameter files for both taxanes and CYP3A4. A $60 \times 60 \times 60$ point grid with a spacing of 0.375 Å centered at -15.0, -17.0, 25.0 was used for the protein model. For other parameters, the default values were selected. The poses with lowest docking energy were selected for analysis.

Results

Identification of cephalomannine metabolites. After cephalomannine was incubated with HLMS and NADPH-generating system, two new peaks were eluted at 6.5 (M-1) and 10.9 min (M-2), respectively (Fig. 2). The new peaks were not observed in the negative controls without NADPH, or without substrate, or without mitochondria. Only the control without NADPH was shown for clarity (Fig. 2).

LC/MS/MS was employed to elucidate the structures of cephalomannine metabolites. Both positive-ion mode and negative-ion mode were examined in the LC/MS. In the positive-ion mode, the following fragments were observed for the cephalomannine (Table 1): m/z 832.7, $[M+H]^+$; m/z 854.9, $[M+Na]^+$; m/z 870.7, $[M+K]^+$; m/z 509.6, i.e. consecutive loss of C13 side chain and acetic acid; m/z 309.8, i.e. consecutive loss of C2 side chain, acetic acid and water on m/z 509.6; m/z 264.6, i.e. C13 side chain; m/z 246.5, i.e. water loss on m/z 264.6. These fragments were in agreement with previous report (Vivekanandan et al., 2006). Characteristic fragment ions of metabolites were 16 mass units greater than that of cephalomannine, indicating that both metabolites were mono-hydroxylated (Table 1). For M-1, m/z 509.3 and 280.2 indicated that the hydroxylation site was in the C13 side chain but not in the taxane core ring (Table 1). For M-2, m/z 525.3, 325.3, and 264.3 implied that hydroxylation site was in the taxane core ring but not in the C2 or C13 side chain (Table 1).

Consistent with previous report (Song et al., 2005), the negative-ion mode provided better sensitivity than the positive-ion mode, therefore negative-ion mode was adopted for MS/MS analysis in current investigation. MS spectra were dominated by

DMD # 18242

$[M+AcO]^-$ in these conditions, therefore $[M+AcO]^-$ was selected as precursor ion to be further fragmented. Fragment ions of cephalomannine (Table 2) included m/z 890.7, $[M+AcO]^-$; m/z 830.7, $[M-H]^-$; m/z 770.6, $[M-AcOH-H]^-$; m/z 525.5 (base peak), $[M-Ac-C13-H]^-$, i.e. consecutive loss of hydrogen, acetyl and C13 side chain breaking C13 ester bond; m/z 373.4, $[525.5-BzOH-HCHO]^-$, i.e. loss of C2 benzoic acid and formaldehyde on m/z 525.5; m/z 262.5, i.e. C13 side chain. For M-1, m/z 278.4 and m/z 525.5 implied that hydroxylation site was in C13 side chain and not in the taxane ring, and the m/z shift from 525.5 to 373.2 excluded benzoate ring at C2 as hydroxylation site (Table 2). Similarly, for M-2, m/z 541.4, 389.6, and 262.3 suggested that the hydroxylation site was in the taxane ring but not in the C13 side chain or C2 benzoate ring (Table 2). The hydroxylation sites deduced from the negative-ion mode were in agreement with that from the positive-ion mode.

The 1H NMR spectra of cephalomannine and its metabolite (M-1) indicated that the phenyls in the C13 side chain were intact (Table 3). In agreement with previous reports (Miller et al., 1981; Chen et al., 2001), the most distinct spectra changes were involved in the tigloylamide group. The 4"-methyl proton signal at 1.73 ppm (3H, d, $J=6.8$ Hz) was replaced by a signal at 4.25 ppm (2H, t, $J=5.6$ Hz). The corresponding 3"-proton signal change from 6.43 ppm (1H, q, $J=7.2$ Hz) to 6.36 ppm (1H, t, $J=6.0$ Hz). These observations suggested that the hydroxylation site was in 4"-methyl group. Another proton signal appeared at 3.70 ppm (1H, t, $J=4.8$ Hz) was assigned to 4"-OH (Table 3). The structure of M-2 (RT=10.9 min) couldn't be ascertained from the fragment ions. In analogy with hydroxylation sites of paclitaxel and some other taxanes

(Cresteil et al., 2002; Frapolli et al., 2006), we propose C6 α as the possible hydroxylation site for M-2 (Fig. 1).

Different metabolism between cephalomannine and paclitaxel. To compare the metabolism between cephalomannine and paclitaxel, we studied the metabolism of two taxanes in five individual human liver samples (H1, H2, H3, H4, and H5), and the results are shown in Fig. 3. For comparison, substrate concentration (10 μ M), microsomal concentration (0.5 mg/mL), and reaction time (30 min) were all kept the same. Under these conditions, there was little difference between cephalomannine and paclitaxel in the overall biotransformation rate (145 *versus* 184 pmol/min/mg). For paclitaxel, 6 α -hydroxypaclitaxel by CYP2C8 was always the dominant product in five liver samples, and the average ratio of the two metabolites hydroxylated at 6 α to C3' was 85:15 (Fig. 3). For cephalomannine, however, 4"-hydroxycephalomannine instead of 6 α -hydroxycephalomannine was the main metabolite in the four out of the five liver samples, and H3 produced about the same amount of the two metabolites (Fig. 3). The average ratio of the two metabolites hydroxylated at 6 α to C4" was 36:64.

To compare species differences, the metabolism of cephalomannine and paclitaxel in RLMs and PLMs was also examined. For cephalomannine, only 4"-hydroxycephalomannine was detected after cephalomannine (50 μ M) was incubated with rat or minipig liver microsomes (0.5 mg/mL) for 30 min (Table 4). 6 α -hydroxycephalomannine was absent in both liver microsomal incubations. For paclitaxel, only 3'-p-hydroxypaclitaxel was detected after paclitaxel (50 μ M) was incubated with RLMs (0.5 mg/mL) for 30 min (Table 4). Neither 3'-p-hydroxypaclitaxel

DMD # 18242

nor 6 α -hydroxypaclitaxel was detected after paclitaxel (50 μ M) was incubated with minipig liver microsomes (0.5 mg/mL) for 30 min (Table 4), although the minipig liver microsomes sample showed high testosterone 6 β -hydroxylation activity (Li et al., 2006).

Chemical inhibition studies. Selective inhibitors of the eight major CYPs were used to screen the CYP isoforms responsible for cephalomannine metabolism in human (Fig. 4). Among tested inhibitors, ketoconazole inhibited the activity of cephalomannine 4"-hydroxylation by about 90%, but didn't inhibit the formation of 6 α -hydroxycephalomannine significantly. Quercetin, on the other hand, inhibited the activity of cephalomannine 6 α -hydroxylation by about 90%, but didn't inhibit the formation of 4"-hydroxycephalomannine remarkably. Inhibitors of other CYP isoforms didn't show significant inhibition (less than 30% inhibition) towards the formation of either metabolite. These results revealed that CYP3A4 was involved in cephalomannine 4"-hydroxylation, and CYP2C8 in 6 α -hydroxylation.

Inhibition of cephalomannine 4"-hydroxylation in RLMs and PLMs by CYP3A, CYP1A, and CYP2C inhibitors is shown in Fig. 5. The inhibitory profiles by selected inhibitors were similar in both RLMs and PLMs incubations system. Both troleandomycin (25 μ M) and ketoconazole (1 μ M) inhibited the activity of cephalomannine 4"-hydroxylation by more than 80%. Furafylline (10 μ M) and sulfaphenazole (10 μ M) exhibited about 10% and 20% inhibition, respectively.

Assay with recombinant human CYPs. To further verify CYP isoforms involved in the metabolism of cephalomannine, activity of cephalomannine hydroxyla-

DMD # 18242

tion was determined using eight cDNA-expressed CYP isoforms (Fig. 6). Cephalomannine 4"-hydroxylation was catalyzed by CYP3A4 (0.66 pmol/min/pmol CYP), and cephalomannine 6 α -hydroxylation was catalyzed by CYP2C8 (1.29 pmol/min/pmol CYP). Other CYP isoforms didn't produce detectable amount of metabolite (less than 0.01 pmol/min/pmol CYP). Therefore, cephalomannine 6 α -hydroxylation was ascribed to CYP2C8, and cephalomannine 4"-hydroxylation was ascribed to CYP3A4.

Molecular Docking. Paclitaxel and cephalomannine were docked to the active site of CYP3A4 (PDB entry 2j0d, Fig. 7). Consistent with experimental data, paclitaxel adopted an orientation in favor of 3'-p-hydroxylation, while cephalomannine adopted an orientation favoring 4"-hydroxylation (Fig. 7). The binding energy didn't differ significantly between paclitaxel (-6.39 kcal/mol) and cephalomannine (-7.61 kcal/mol). The amino acid residues Arg¹⁰⁶, Phe¹⁰⁸, Ser¹¹⁹, Phe³⁰⁴, Ala³⁰⁵, Phe²¹³, Gly⁴⁸¹, and Leu⁴⁸² showed interactions with paclitaxel, while the amino acid residues interacting with cephalomannine were Arg¹⁰⁵, Phe²¹³, Phe³⁰⁴, Glu³⁰⁸, Thr³⁰⁹, Ala³⁷⁰, and Leu⁴⁸².

Kinetic characteristics of cephalomannine and paclitaxel metabolism. In H1 liver microsomes, formation rates of cephalomannine and paclitaxel metabolites were linear up to 0.5 mg/mL microsomal protein and 30 min. Thus, 0.5 mg/mL HLMs and 30 min were adopted in the following kinetic assay. The formation of cephalomannine and paclitaxel metabolites in liver microsomes and recombinant CYPs obeyed the Michaelis-Menten kinetics. The kinetic parameters, K_m and V_m for cephalomannine

DMD # 18242

and paclitaxel oxidation were listed in Table 4 and results of typical kinetic experiments of cephalomannine were graphically displayed in Fig. 8. The K_m values of paclitaxel 6 α - and 3'-p-hydroxylation were similar (13 *versus* 17 μ M), but the values of their V_m showed about 3-fold difference (233 *versus* 84 pmol/min/mg). The catalytic efficiency of 6 α -hydroxylation, as measured by V_m/K_m , was about 3-fold higher than 3'-p-hydroxylation (17 *versus* 5). On the other hand, cephalomannine 6 α - and 4"-hydroxylation showed about 3-fold difference in their K_m values (52 *versus* 16 μ M) despite that the V_m values were similar (234 *versus* 275 pmol/min/mg). The catalytic efficiency of 6 α -hydroxylation, as reflected by V_m/K_m , was 4-fold lower than 4"-hydroxylation (4 *versus* 17).

In RLMs, the values of K_m towards cephalomannine and paclitaxel differed only slightly (15 *versus* 21 μ M, Table 4). The 12-fold difference in their V_m values (1853 *versus* 153 pmol/min/mg) made RLMs metabolized cephalomannine much more efficiently than paclitaxel (V_m/K_m value, 125 *versus* 7). In PLMs, the K_m and V_m values for cephalomannine 4"-hydroxylation were 11 μ M and 108 pmol/min/mg (Table 4), and the catalytic efficiency of cephalomannine was about 10-fold lower in PLMs than in RLMs (V_m/K_m value, 10 *versus* 125).

Kinetic parameters of cephalomannine and paclitaxel metabolism in recombinant CYP3A4 and CYP2C8 are shown in Table 5. CYP3A4 catalyzed cephalomannine more efficiently than paclitaxel (V_m/K_m value, 195 *versus* 16) mainly by an increased V_m (1600 *versus* 91 pmol/min/nmol CYP). On the other hand, increased K_m (33 *versus* 8.5 μ M) made CYP2C8 transform cephalomannine less efficiently than paclitaxel

DMD # 18242

(V_m/K_m value, 150 *versus* 221).

Taxanes are known to be hydrophobic compounds, and the aqueous solubility of paclitaxel is 35 μM (Swindell et al., 1991). The addition of 1% methanol increases the solubility slightly. The solubility limitation makes it impossible to extend the substrate concentration further to cover the range of five-fold K_m value. Therefore, the K_m might be overestimated and the resulting intrinsic clearance might be inaccurate because of the narrow substrate concentration range.

Discussion

CYP-mediated oxidative metabolism represented the major excretion pathway for paclitaxel in both human and rat, with only 10% of paclitaxel was excreted as unchanged drug (Anderson et al., 1995; Cresteil et al., 2002). 10-acetyl and C13 side chain were found to affect taxane's regioselective oxidation (Cresteil et al., 2002). However, more evidences indicated that the regioselective hydroxylation was determined by the substituents at C3' (Frapolli et al., 2006; Gut et al., 2006). Many of the new generation taxanes had modified substituents at C3' compared with paclitaxel, such as BAY59-8862 (Sano et al., 2006), IDN5390 (Ferlini et al., 2005), BMS-275183 (Broker et al., 2007), MAC-321 (Lockhart et al., 2007), and SB-T-1102 (Ojima et al., 1996). It would be helpful to synthesize metabolism-stable taxanes if we knew how substituents at C3' affected taxane's metabolism. Therefore, we selected a pair of analogue slightly different only at C3', cephalomannine and paclitaxel, to evaluate the effect of slight structure change on metabolism.

In the incubation system with HLMs, two cephalomannine metabolites (M-1, M-2) were detected, and M-1 was identified to be 4"-hydroxycephalomannine. Mass spectra suggested that the hydroxylation site of M-2 was in the taxane core ring, but not in the C2 or C13 side chain, nor in the acetyls at C4 or C10. C6 α was proposed as the possible hydroxylation site for M-2. Chemical inhibition studies and assays with recombinant human CYPs indicated that 4"-hydroxycephalomannine was produced predominantly by CYP3A4 and 6 α -hydroxycephalomannine by CYP2C8. In five different human liver samples, cephalomannine 6 α -hydroxylation correlated with paclitaxel

DMD # 18242

6 α -hydroxylation (CYP2C8, $R^2=0.95$), and cephalomannine 4"-hydroxylation correlated with paclitaxel 3'-p-hydroxylation (CYP3A4, $R^2=0.96$). Relative poor correlations were found between paclitaxel 6 α -hydroxylation (CYP2C8) and paclitaxel 3'-p-hydroxylation (CYP3A4, $R^2=0.64$), and between cephalomannine 6 α -hydroxylation and cephalomannine 4"-hydroxylation ($R^2=0.40$). These results were in agreement with M-1 was produced by CYP3A4, and M-2 was by CYP2C8.

In humans, paclitaxel was primarily hydroxylated by CYP2C8 at C6 α and secondly by CYP3A4 at C3' (Harris et al., 1994). Although 3'-p-hydroxypaclitaxel could be the dominant metabolite in certain cases (Desai et al., 1998; Taniguchi et al., 2005), 6 α -hydroxypaclitaxel was generally regarded as the major product, and the ratio of two metabolites hydroxylated at C6 α to C3' was about 80:20 in HLMs (Venkatakrishnan et al., 2003; Taniguchi et al., 2005). This result was in agreement with present study, in which the average ratio of paclitaxel metabolites hydroxylated at C6 α to C3' in five liver microsomes was 85:15 (Fig. 3). For cephalomannine, on the other hand, the average ratio of the two metabolites hydroxylated at 6 α to C4" was 36:64 in the same panel of liver samples (Fig. 3). Therefore, the main hydroxylation site transferred from C6 α to C4", and the main metabolizing CYP for cephalomannine changed from CYP2C8 to CYP3A4 compared with paclitaxel. In vitro antitumor activity of 4"-hydroxycephalomannine was more than 60-fold less potent than cephalomannine (Chen et al., 2001), therefore cephalomannine 4"-hydroxylation could be regarded as a detoxification process.

From kinetics of paclitaxel and cephalomannine hydroxylation (Table 4 and Table

DMD # 18242

5), it can be concluded that the presence of a tigloyl group instead of a benzoyl group at C3' reduces the contribution of CYP2C8 via decreasing the affinity for the protein. It probably indicates that the hydrophobic interactions with CYP2C8 peptide chain as suggested before (Cresteil et al., 2002) decrease when the benzoyl is replaced by the tigloyl. On the other hand, the replacement of benzamide by tigloylamide increases the overall metabolism by CYP3A via an increased V_m in human, rat and minipig liver microsomes and recombinant CYP3A4 (Table 4 and Table 5). This may imply that alkyl is more susceptible to CYP3A hydroxylation than phenyl in the amide part of taxane. During P450 catalytic cycle, the target C—H bond would break and form radicals before oxygen was added (Porter and Coon, 1991). The bond dissociation energy (DH) of C—H bond at C4" ($\text{CH}_3\text{C}=\text{CHCH}_2\text{—H}$, $\text{DH}\approx 88.8$ kcal/mol) in cephalomannine is lower than that at 3'-p-phenyl ($\text{C}_6\text{H}_4\text{—H}$, $\text{DH}\approx 109$ kcal/mol) in paclitaxel (Blanksby and Ellison, 2003), which gives cephalomannine a lower activation energy. When the activation energy decreases, the rate constant would increase according to the Arrhenius equation. Thus the rate of cephalomannine 4"-hydroxylation is faster than that of paclitaxel 3'-p-hydroxylation.

In contrast to paclitaxel, C4" instead of 3'-p-phenyl in cephalomannine is hydroxylated. Molecular docking suggests the regioselective metabolism of paclitaxel and cephalomannine at C3' is determined by the ligand and receptor interaction. Another possible explanation is the difference in the DH values. As discussed earlier, substituent with a lower C—H DH value is more susceptible to CYP oxidation, as it needs lower activation energy. The DH of C—H at C4" is lower than that at

DMD # 18242

3'-p-phenyl, thus C4" instead of 3'-p-phenyl in cephalomannine is hydroxylated. The same rationale can also explain the observations that the *tert*-butyl ($\text{OC}(\text{CH}_3)_2\text{CH}_2\text{—H}$, $\text{DH}\approx 101$ kcal/mol) but not the phenyl ($\text{C}_6\text{H}_4\text{—H}$, $\text{DH}\approx 109$ kcal/mol) at C3' of docetaxel is hydroxylated by CYP3A4 (Cresteil et al., 2002), and the isobutyl ($((\text{CH}_3)_2\text{C—H}$, $\text{DH}\approx 98.6$ kcal/mol) or the isobutenyl ($\text{CH=CCH}_2\text{—H}$, $\text{DH}\approx 88.8$ kcal/mol) instead of the *tert*-butyl ($\text{OC}(\text{CH}_3)_2\text{CH}_2\text{—H}$, $\text{DH}\approx 101$ kcal/mol) is hydroxylated in SB-T-1102, SB-T-1214, SB-T-1216 (Gut et al., 2006), and IDN5390 (Frapolli et al., 2006). It should be noted that we neglected other aspects such as steric hindrance, structure modifications at C10, and influence of nearby functional groups, which may also contribute the regioselective metabolism.

Similar to the metabolism of paclitaxel (Vaclavikova et al., 2004), species differences in cephalomannine metabolism were observed, and 6 α -hydroxycephalomannine was missing in the incubation system of RLMs and PLMs. The main metabolites of paclitaxel varied a lot among different species (Vaclavikova et al., 2004), but for cephalomannine, 4"-hydroxycephalomannine was the main metabolite in HLMs, RLMs, and PLMs. In RLMs and PLMs, the activity of cephalomannine 4"-hydroxylation was strongly inhibited by CYP3A inhibitors troleandomycin and ketoconazole. These observations suggested that human CYP3A4 orthologs in minipig (CYP3A29) and rat (CYP3A1/2) might play a major role in cephalomannine metabolism; however, detailed examinations with recombinant rat and minipig CYPs were needed to ascribe the reaction to particular animal CYP isoforms.

In conclusion, the major hydroxylation site and primary CYP isoform are quite

DMD # 18242

different between cephalomannine and paclitaxel despite their structure similarity. Like paclitaxel, C6 α of cephalomannine is still the hydroxylation site, whereas the major hydroxylation site transfers to C4" in the side chain and CYP3A4 instead of CYP2C8 becomes the main metabolism enzyme. Our results demonstrate that relative minor modification of taxane at C3' has major consequence on its metabolism, and taxane's C3' substituent with a lower C—H DH value is more susceptible to CYP oxidation.

DMD # 18242

Acknowledgement

We thank Dr. Ning Zhu from The Second Affiliated Hospital of Dalian Medical University, and Jia-Ning Qian from Chemistry Department, University of Toronto for proofreading our manuscript. We gratefully acknowledged Dr. Hong Wei from The Third Military Medical University of China for the generous gift of minipig livers.

References

- Anderson CD, Wang J, Kumar GN, McMillan JM, Walle UK and Walle T (1995)
Dexamethasone induction of taxol metabolism in the rat. *Drug Metab Dispos*
23:1286-1290.
- Anzenbacher P, Soucek P, Anzenbacherova E, Gut I, Hruby K, Svoboda Z and Kvet-
ina J (1998) Presence and activity of cytochrome P450 isoforms in minipig
liver microsomes. Comparison with human liver samples. *Drug Metab Dispos*
26:56-59.
- Barboni L, Ballini R, Giarlo G, Appendino G, Fontana G and Bombardelli E (2005)
Synthesis and biological evaluation of methoxylated analogs of the newer
generation taxoids IDN5109 and IDN5390. *Bioorg Med Chem Lett*
15:5182-5186.
- Bhalla KN, Kumar GN, Walle UK, Ibrado AM, Javed T, Stuart RK, Reed C, Arbuck
SG and Walle T (1999) Phase I and pharmacologic study of a 3-hour infusion
of paclitaxel followed by cisplatin and 5-fluorouracil in patients with ad-
vanced solid tumors. *Clin Cancer Res* **5**:1723-1730.
- Bjornsson TD, Callaghan JT, Einolf HJ, Fischer V, Gan L, Grimm S, Kao J, King SP,
Miwa G, Ni L, Kumar G, McLeod J, Obach SR, Roberts S, Roe A, Shah A,
Snikeris F, Sullivan JT, Tweedie D, Vega JM, Walsh J and Wrighton SA (2003)
The conduct of in vitro and in vivo drug-drug interaction studies: a PhRMA
perspective. *J Clin Pharmacol* **43**:443-469.
- Blanksby SJ and Ellison GB (2003) Bond dissociation energies of organic molecules.

DMD # 18242

Acc Chem Res **36**:255-263.

Broker LE, Veltkamp SA, Heath EI, Kuenen BC, Gall H, Astier L, Parker S, Kayitalire L, Lorusso PM, Schellens JH and Giaccone G (2007) A phase I safety and pharmacologic study of a twice weekly dosing regimen of the oral taxane BMS-275183. *Clin Cancer Res* **13**:3906-3912.

Chen TS, Li XH, Bollag D, Liu YC and Chang CJ (2001) Biotransformation of taxol. *Tetrahedron Lett* **42**:3787-3789.

Cresteil T, Monsarrat B, Dubois J, Sonnier M, Alvinerie P and Gueritte F (2002) Regioselective metabolism of taxoids by human CYP3A4 and 2C8: structure-activity relationship. *Drug Metab Dispos* **30**:438-445.

Desai PB, Duan JZ, Zhu YW and Kouzi S (1998) Human liver microsomal metabolism of paclitaxel and drug interactions. *Eur J Drug Metab Pharmacokinet* **23**:417-424.

Ekroos M and Sjogren T (2006) Structural basis for ligand promiscuity in cytochrome P450 3A4. *Proc Natl Acad Sci U S A* **103**:13682-13687.

Ferlini C, Raspaglio G, Mozzetti S, Cicchillitti L, Filippetti F, Gallo D, Fattorusso C, Campiani G and Scambia G (2005) The seco-taxane IDN5390 is able to target class III beta-tubulin and to overcome paclitaxel resistance. *Cancer Res* **65**:2397-2405.

Frapolli R, Marangon E, Zaffaroni M, Colombo T, Falcioni C, Bagnati R, Simone M, D'Incalci M, Manzotti C, Fontana G, Morazzoni P and Zucchetti M (2006) Pharmacokinetics and metabolism in mice of IDN 5390

DMD # 18242

(13-(N-Boc-3-i-butyloxyserinoyl)-C-7,8-seco-10-deacetylbaccatin III), a new oral c-seco-taxane derivative with antiangiogenic property effective on paclitaxel-resistant tumors. *Drug Metab Dispos* **34**:2028-2035.

Gut I, Ojima I, Vaclavikova R, Simek P, Horsky S, Linhart I, Soucek P, Kondrova E, Kuznetsova LV and Chen J (2006) Metabolism of new-generation taxanes in human, pig, minipig and rat liver microsomes. *Xenobiotica* **36**:772-792.

Harris JW, Rahman A, Kim BR, Guengerich FP and Collins JM (1994) Metabolism of taxol by human hepatic microsomes and liver slices: participation of cytochrome P450 3A4 and an unknown P450 enzyme. *Cancer Res* **54**:4026-4035.

Helson L and Ainsworth SK (1997) Method for assessing sensitivity of tumor cells to cephalomannine and 10-deacetyltaxol, US patent 5688517 (1997 November 18).

Huang SM, Temple R, Throckmorton DC and Lesko LJ (2007) Drug interaction studies: study design, data analysis, and implications for dosing and labeling. *Clin Pharmacol Ther* **81**:298-304.

Kobayashi K, Urashima K, Shimada N and Chiba K (2003) Selectivities of human cytochrome P450 inhibitors toward rat P450 isoforms: study with cDNA-expressed systems of the rat. *Drug Metab Dispos* **31**:833-836.

Li J, Liu Y, Zhang JW, Wei H and Yang L (2006) Characterization of hepatic drug-metabolizing activities of Bama miniature pigs (*Sus scrofa domestica*): comparison with human enzyme analogs. *Comp Med* **56**:286-290.

Lockhart AC, Bukowski R, Rothenberg ML, Wang KK, Cooper W, Grover J, Apple-

DMD # 18242

- man L, Mayer PR, Shapiro M and Zhu AX (2007) Phase I trial of oral
 MAC-321 in subjects with advanced malignant solid tumors. *Cancer Chemo-
 ther Pharmacol* **60**:203-209.
- Lowry OH, Rosebrough NJ, Farr AL and Randall RJ (1951) Protein measurement
 with the Folin phenol reagent. *J Biol Chem* **193**:265-275.
- Mastalerz H, Cook D, Fairchild CR, Hansel S, Johnson W, Kadow JF, Long BH, Rose
 WC, Tarrant J, Wu MJ, Xue MQ, Zhang G, Zoeckler M and Vyas DM (2003)
 The discovery of BMS-275183: an orally efficacious novel taxane. *Bioorg
 Med Chem* **11**:4315-4323.
- Miller RW, Powell RG, Smith CR, Arnold E and Clardy J (1981) Antileukemic alka-
 loids from *Taxus wallichiana* Zucc. *J. Org. Chem.* **46**:1469-1474.
- Morris GM, Goodsell DS, Halliday RS, Huey R, Hart WE, Belew RK and Olson AJ
 (1998) Automated docking using a Lamarckian genetic algorithm and an em-
 pirical binding free energy function. *J Comput Chem* **19**:1639-1662.
- Mroczek T, Glowinski K and Hajnos M (2000) Screening for pharmaceutically impor-
 tant taxoids in *Taxus baccata* var. *Aurea* corr. with CC/SPE/HPLC-PDA pro-
 cedure. *Biomed Chromatogr* **14**:516-529.
- Ojima I, Slater JC, Michaud E, Kuduk SD, Bounaud PY, Vrignaud P, Bissery MC,
 Veith JM, Pera P and Bernacki RJ (1996) Syntheses and structure-activity re-
 lationships of the second-generation antitumor taxoids: exceptional activity
 against drug-resistant cancer cells. *J Med Chem* **39**:3889-3896.
- Omura T and Sato R (1964) The Carbon Monoxide-Binding Pigment of Liver Micro-

DMD # 18242

- somes. I. Evidence for Its Hemoprotein Nature. *J Biol Chem* **239**:2370-2385.
- Porter TD and Coon MJ (1991) Cytochrome P-450. Multiplicity of isoforms, substrates, and catalytic and regulatory mechanisms. *J Biol Chem* **266**:13469-13472.
- Sanner MF (1999) Python: a programming language for software integration and development. *J Mol Graph Model* **17**:57-61.
- Sano D, Matsuda H, Ishiguro Y, Nishimura G, Kawakami M and Tsukuda M (2006) Antitumor effects of IDN5109 on head and neck squamous cell carcinoma. *Oncol Rep* **15**:329-334.
- Shi Q, Wang HK, Bastow KF, Tachibana Y, Chen K, Lee FY and Lee KH (2001) Antitumor agents 210. Synthesis and evaluation of taxoid-epipodophyllotoxin conjugates as novel cytotoxic agents. *Bioorg Med Chem* **9**:2999-3004.
- Singla AK, Garg A and Aggarwal D (2002) Paclitaxel and its formulations. *Int J Pharm* **235**:179-192.
- Song L, Prey JD, Xue J, Kanter P, Manzotti C, Bombardelli E, Morazzoni P and Pendyala L (2005) Pharmacokinetic measurements of IDN 5390 using electrospray ionization tandem mass spectrometry: structure characterization and quantification in dog plasma. *Rapid Commun Mass Spectrom* **19**:3617-3625.
- Sparreboom A, van Asperen J, Mayer U, Schinkel AH, Smit JW, Meijer DK, Borst P, Nooijen WJ, Beijnen JH and van Tellingen O (1997) Limited oral bioavailability and active epithelial excretion of paclitaxel (Taxol) caused by P-glycoprotein in the intestine. *Proc Natl Acad Sci U S A* **94**:2031-2035.

DMD # 18242

- Spratlin J and Sawyer MB (2007) Pharmacogenetics of paclitaxel metabolism. *Crit Rev Oncol Hematol* **61**:222-229.
- Swindell CS, Krauss NE, Horwitz SB and Ringel I (1991) Biologically active taxol analogues with deleted A-ring side chain substituents and variable C-2' configurations. *J Med Chem* **34**:1176-1184.
- Taniguchi R, Kumai T, Matsumoto N, Watanabe M, Kamio K, Suzuki S and Kobayashi S (2005) Utilization of human liver microsomes to explain individual differences in paclitaxel metabolism by CYP2C8 and CYP3A4. *J Pharmacol Sci* **97**:83-90.
- Vaclavikova R, Soucek P, Svobodova L, Anzenbacher P, Simek P, Guengerich FP and Gut I (2004) Different in vitro metabolism of paclitaxel and docetaxel in humans, rats, pigs, and minipigs. *Drug Metab Dispos* **32**:666-674.
- Venkatakrisnan K, von Moltke LL, Obach RS and Greenblatt DJ (2003) Drug metabolism and drug interactions: application and clinical value of in vitro models. *Curr Drug Metab* **4**:423-459.
- Vivekanandan K, Swamy MG, Prasad S, Mukherjee R and Burman AC (2006) Identification of isocephalomannine in the presence of cephalomannine isomers and alkali metal ion adducts in a paclitaxel active pharmaceutical ingredient using electrospray tandem mass spectrometry. *Rapid Commun Mass Spectrom* **20**:1731-1735.

DMD # 18242

Footnotes

This work was supported by the 973 Program (2003CB716005) of the Ministry of Science and Technology of China, the National Natural Science Foundation of China (30640066) and DICP Innovation Fund of Chinese Academy of Sciences.

Author for correspondence: Dr. & Prof. Ling Yang, Laboratory of Pharmaceutical Resource Discovery, Dalian Institute of Chemical Physics, Chinese Academy of Sciences, NO.457 Zhongshan Road, Dalian, 116023 China, E-mail: yling@dicp.ac.cn

DMD # 18242

Figure legends

Figure 1. Structure of paclitaxel (A) and cephalomannine (B). Arrows denote identified hydroxylation sites in paclitaxel or proposed hydroxylation sites in cephalomannine.

Figure 2. Representative HPLC profiles of cephalomannine and its metabolites. Cephalomannine (60 μ M) was incubated with HLMs (1.0 mg/mL) at 37 °C for 60 min with (+NADPH) or without (-NADPH) NADPH-generating system as described in Materials and Methods. Metabolites (M-1 and M-2) and cephalomannine were eluted at 6.5, 10.9, and 14.1 min, respectively.

Figure 3. Different metabolism of cephalomannine and paclitaxel in microsomes from five different human liver samples (H1, H2, H3, H4, and H5). Cephalomannine (10 μ M) or paclitaxel (10 μ M) was incubated with liver microsomes (0.5mg/mL) for 30 min. Mean \pm SD of duplicate incubations.

Figure 4. Inhibition of cephalomannine metabolism by selective P450 inhibitors in HLMs. The selective inhibitors (or substrates) and their concentrations were as follows: furafylline (10 μ M) for CYP1A2, 8-methoxypsoralen (2.5 μ M) for CYP2A6, quercetin (20 μ M) CYP2C8, sulfaphenazole (10 μ M) for CYP2C9, S-mephenytoin (100 μ M) for CYP2C19, quinidine (10 μ M) for CYP2D6, clomethiazole (50 μ M) for CYP2E1, ketoconazole (1 μ M) for CYP3A4. Mean \pm SD of duplicate incubations.

DMD # 18242

Figure 5. Inhibition of cephalomannine metabolism in RLMs and PLMs. Inhibitors and their concentrations were as follows: troleandomycin (25 μ M), ketoconazole (1 μ M), sulfaphenazole (10 μ M), and furafylline (10 μ M). Mean \pm SD of duplicate incubations.

Figure 6. Cephalomannine hydroxylation by cDNA-expressed P450 isoforms. Cephalomannine (60 μ M) was incubated with each of the recombinant CYPs (40-80 pmol of CYP/mL) at 37°C for 60 min. Mean \pm SD of duplicate incubations.

Figure 7. Docking of paclitaxel (A, binding energy -6.39 kcal/mol) and cephalomannine (B, binding energy -7.61 kcal/mol) to the active site of CYP3A4 (PDB entry, 2j0d)

Figure 8. Michael-Menten plots (A) and Lineweaver-Burk plots (B) of cephalomannine hydroxylation in H1 liver microsomes. Cephalomannine (4.0-70 μ M) was incubated with HLMs (0.5mg/mL) at 37 °C for 30 min with NADPH-generating system.

DMD # 18242

Table 1. Positive-ion LC/MS fragmentations of cephalomannine and its two metabolites (M-1 and M-2).

Compounds	RT (min)	Fragments
M-1	6.5	886.3, 870.4, 848.4, 509.3, 309.4, 280.2, 262.2
M-2	10.9	886.3, 870.3, 848.2, 525.3, 325.3, 264.3, 246.2
Cephalomannine	14.1	870.7, 854.9, 832.7, 509.6, 309.8, 264.6, 246.5

DMD # 18242

Table 2. Negative-ion LC/MS/MS fragmentations of cephalomannine and its two metabolites (M-1 and M-2).

Compounds	RT (min)	Precursor ion	Product ions (Base peak in bold)
M-1	6.5	906.6	846.6, 786.4, 525.5 , 373.2, 278.4
M-2	10.9	906.6	846.5, 786.8, 541.4 , 389.6, 262.3
Cephalomannine	14.1	890.7	830.6, 770.6, 525.5 , 373.4, 262.5

DMD # 18242

Table 3. ¹HNMR data for cephalomannine and its metabolite (M-1).

Cephalomannine	M-1	Position
8.12 (2H, dd, J=8.4, 1.2)	8.12 (2H, dd, J=7.2, 1.6)	<i>o</i> -H of OBz
7.62 (1H, tt, J=7.6, 1.2)	7.62 (1H, t, J=7.2)	<i>p</i> -H of OBz
7.51 (2H, t, J=7.6)	7.51 (2H, t, J=8)	<i>m</i> -H of OBz
7.42 (2H, br s)	7.42 (2H, br s)	<i>o</i> -H of 3'-Ph
7.41 (2H, br s)	7.41 (2H, br s)	<i>m</i> -H of 3'-Ph
7.34 (1H, m, J=4.0)	7.35 (1H, m, J=4.8)	<i>p</i> -H of 3'-Ph
6.51 (1H, d, J=8.8)	6.65 (1H, d, J=8.8)	NH
6.43 (1H, q, J=7.2)	6.36 (1H, t, J=6.0)	3''-H
6.27 (1H, s)	6.27 (1H, s)	10-H
6.21 (1H, br t, J=9.2)	6.24 (1H, br t, J=8.8)	13-H
5.67 (1H, d, J=7.2)	5.67 (1H, d, J=6.8)	2-H
5.61 (1H, dd, J=8.8, 2.8)	5.63 (1H, dd, J=9.2, 2.8)	3'-H
4.94 (1H, dd, J=9.6, 2.0)	4.94 (1H, dd, J=10.0, 1.2)	5-H
4.71 (1H, d, J=2.8)	4.72 (1H, d, J=2.8)	2'-H
4.40 (1H, dd, J=10.8, 6.8)	4.40 (1H, dd, J=10.4, 6.8)	7-H
4.30 (1H, d, J=8.8)	4.30 (1H, d, J=8.4)	20-H
—	4.25 (2H, t, J=5.6)	4''-H
4.19 (1H, d, J=8.8)	4.19 (1H, d, J=8.4)	20-H
3.79 (1H, d, J=6.8)	3.79 (1H, d, J=6.8)	3-H

DMD # 18242

—	3.70 (1H, t, J=4.8)	4''-OH
3.49 (1H, s)	3.64 (1H, s)	
2.55 (1H, m)	2.55 (1H, m)	6-H
2.36 (3H, s)	2.38 (3H, s)	10-OCOCH ₃
2.30 (2H, m)	2.32 (2H, m)	14-H
2.25 (3H, s)	2.25 (3H, s)	4-OCOCH ₃
1.89 (1H, m)	1.89 (1H, m)	6-H
1.80 (3H, s)	1.80 (3H, s)	18-CH ₃
1.80 (3H, s)	1.80 (3H, s)	2''-CH ₃
1.73 (3H, d, J=6.8)	—	4''-CH₃
1.68 (3H, s)	1.68 (3H, s)	19-CH ₃
1.26 (3H, s)	1.26 (3H, s)	16-CH ₃
1.15 (3H, s)	1.15 (3H, s)	17-CH ₃

Notes: a) Chemical shifts are expressed in *ppm* and coupling constants in Hz.

b) s, singlet; d, doublet; dd, double doublet; t, triplet; tt, triple triplet; q, quadruplet; br s, broad singlet; m, multiplet.

Table 4. Kinetic parameters of cephalomannine and paclitaxel metabolism in HLMs, RLMs, and PLMs^a.

Taxane	Metabolite	HLM ^b			RLM			PLM		
		K _m	V _m	V _m /K _m	K _m	V _m	V _m /K _m	K _m	V _m	V _m /K _m
		μM	pmol/min/mg		μM	pmol/min/mg		μM	pmol/min/mg	
Cephalomannine	6α	52	234	4	N.D.	N.D.	N.D.	N.D.	N.D.	N.D.
	C4"	16	275	17	15	1853	124	11	108	10
Paclitaxel	6α	13	233	17	N.D.	N.D.	N.D.	N.D.	N.D.	N.D.
	C3'	17	84	5	21	153	7	N.D.	N.D.	N.D.

^aN.D., not detected.^bKinetic parameters were estimated from H1 liver microsomes.

Table 5. Kinetic parameters of cephalomannine and paclitaxel metabolism in recombinant CYP3A4 and CYP2C8^a.

Taxane	Metabolite	CYP3A4			CYP2C8		
		K _m	V _m	V _m /K _m	K _m	V _m	V _m /K _m
		μM	pmol/min/nmol P450		μM	pmol/min/nmol P450	
Cephalomannine	6α	N.D.	N.D.	N.D.	33	4900	150
	C4"	8.2	1600	195	N.D.	N.D.	N.D.
Paclitaxel	6α	N.D.	N.D.	N.D.	8.5	1900	221
	C3'	5.8	91	16	N.D.	N.D.	N.D.

^aN.D., not detected

Fig.1

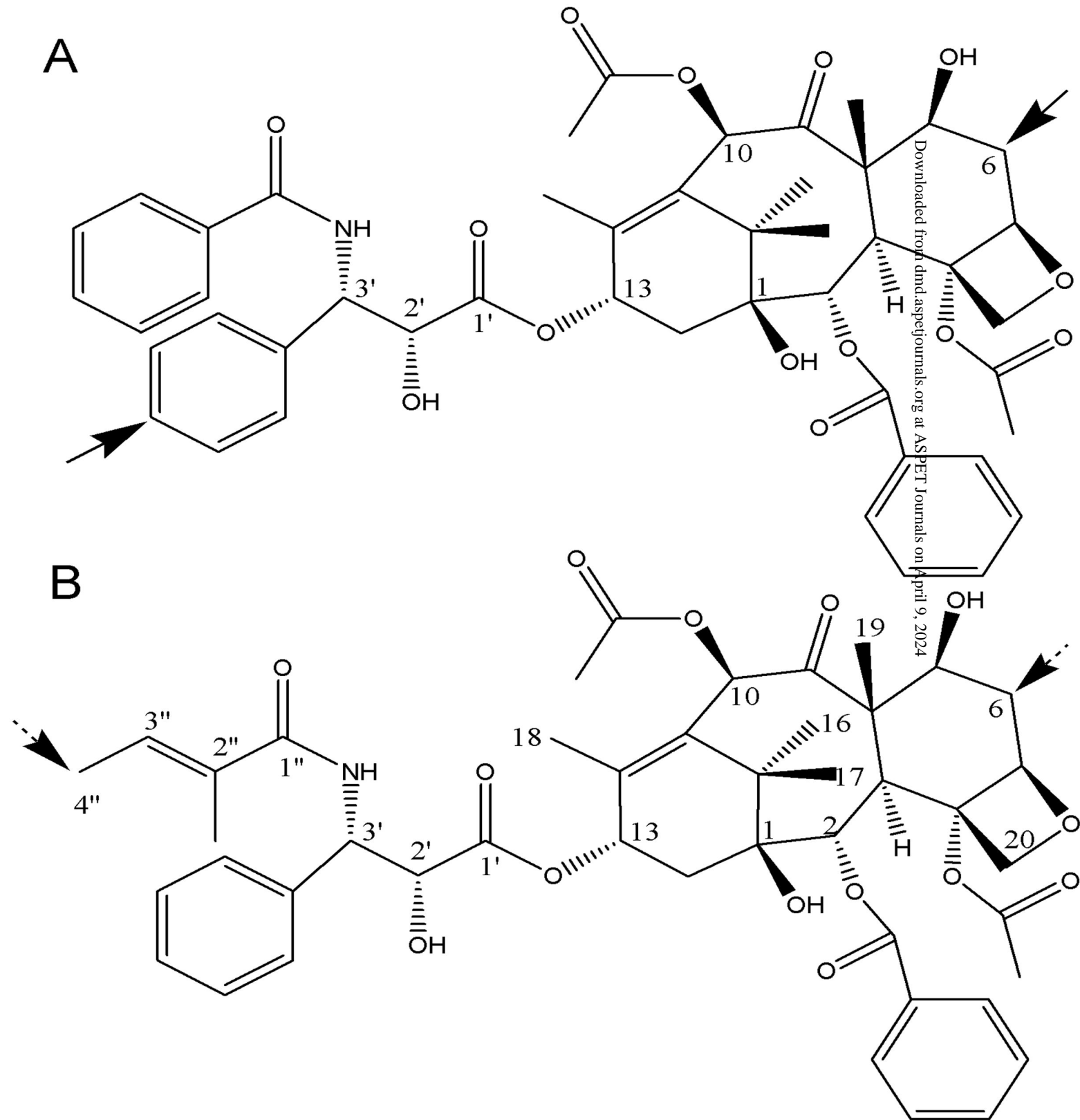


Fig.2

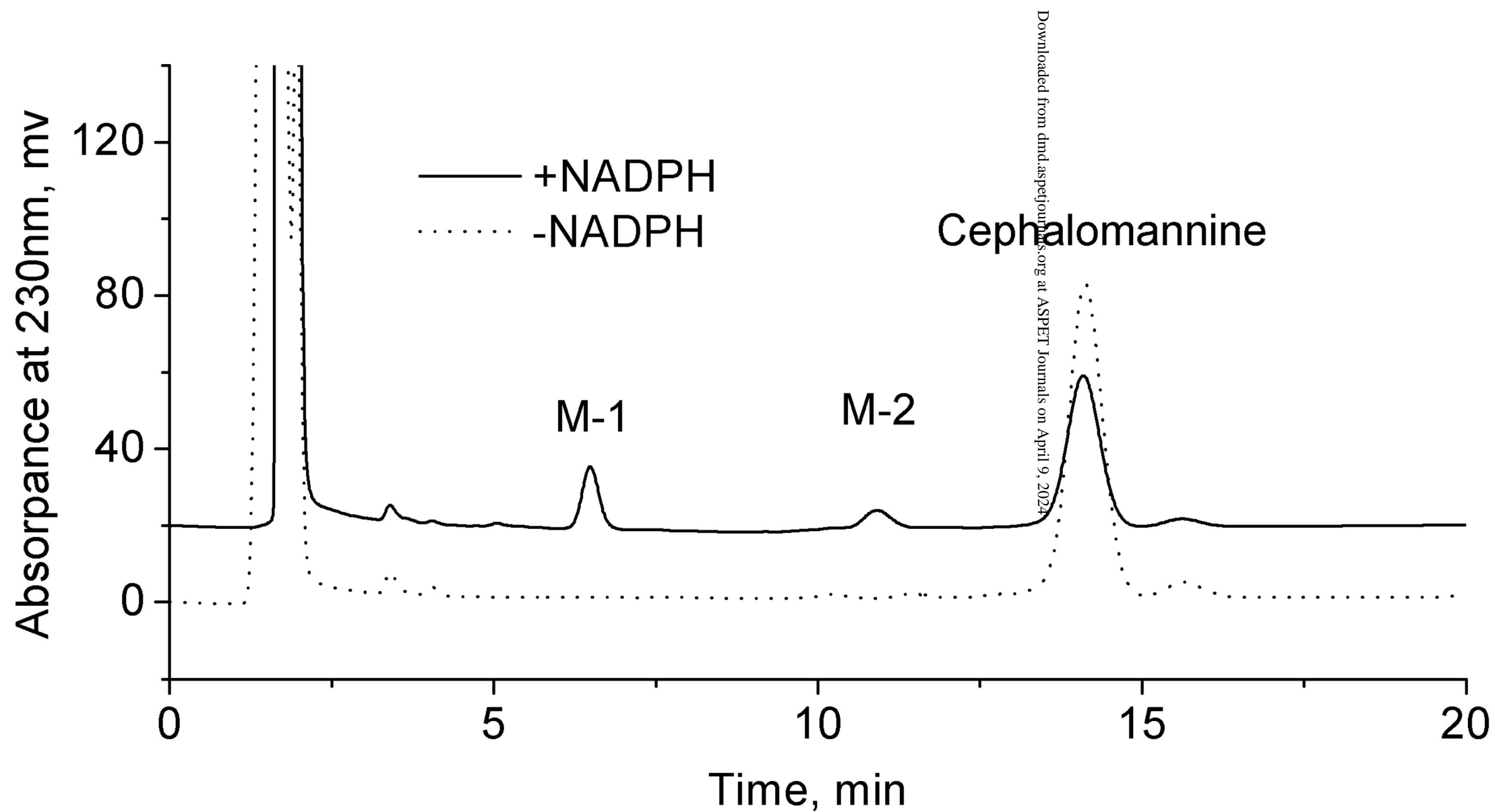
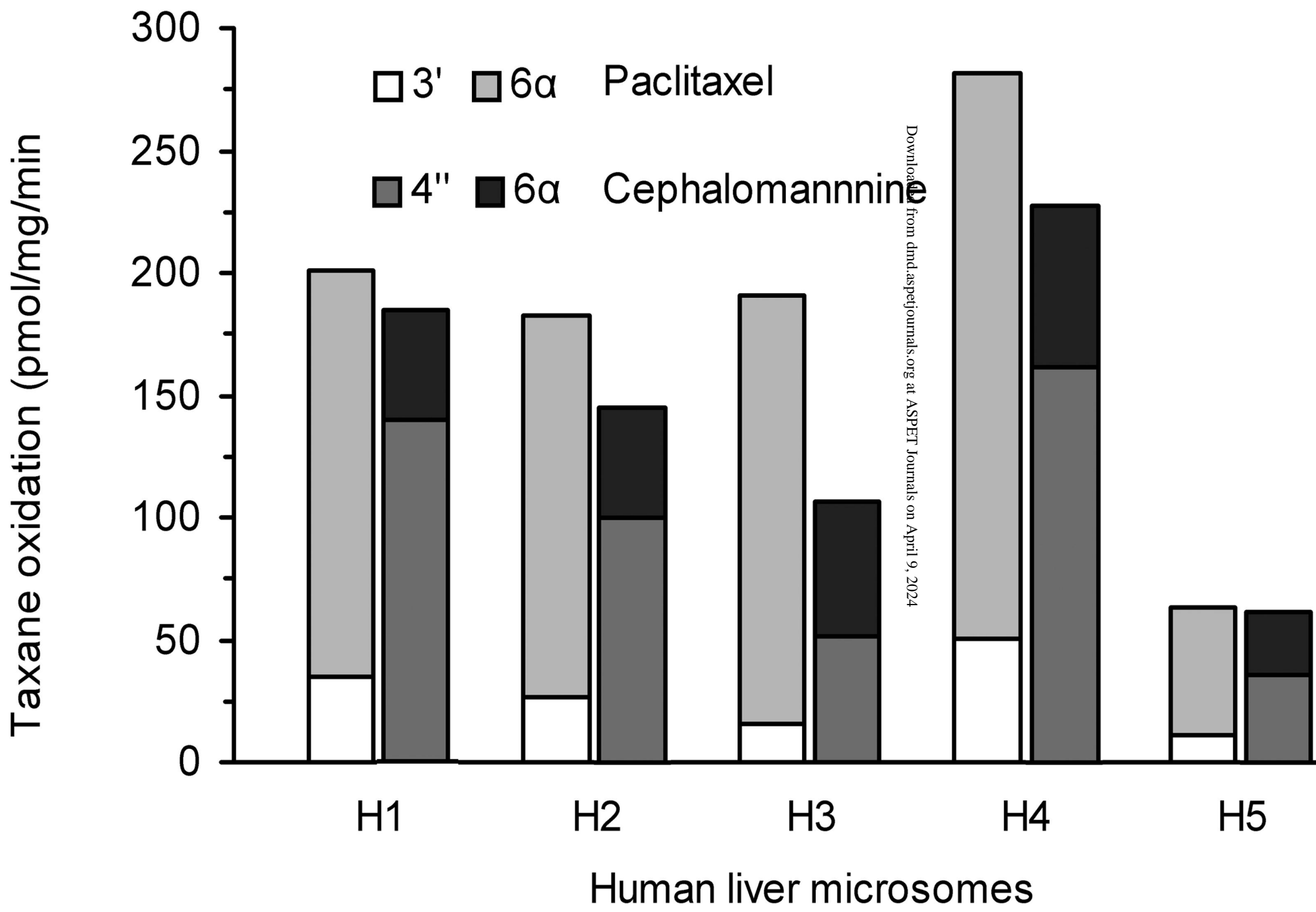


Fig.3



Downloaded from dmd.aspetjournals.org at ASPET Journals on April 9, 2024

Fig.4

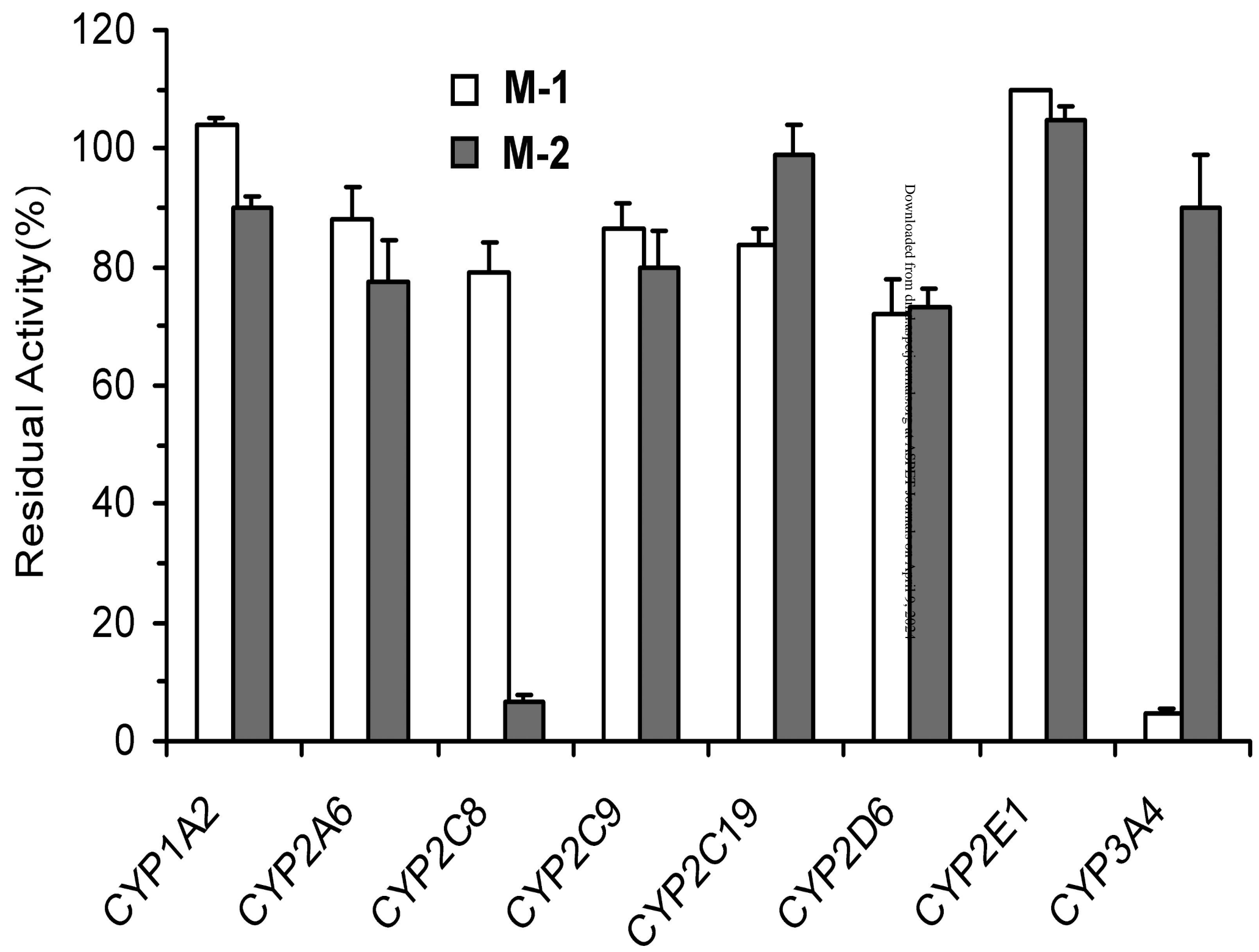


Fig.5

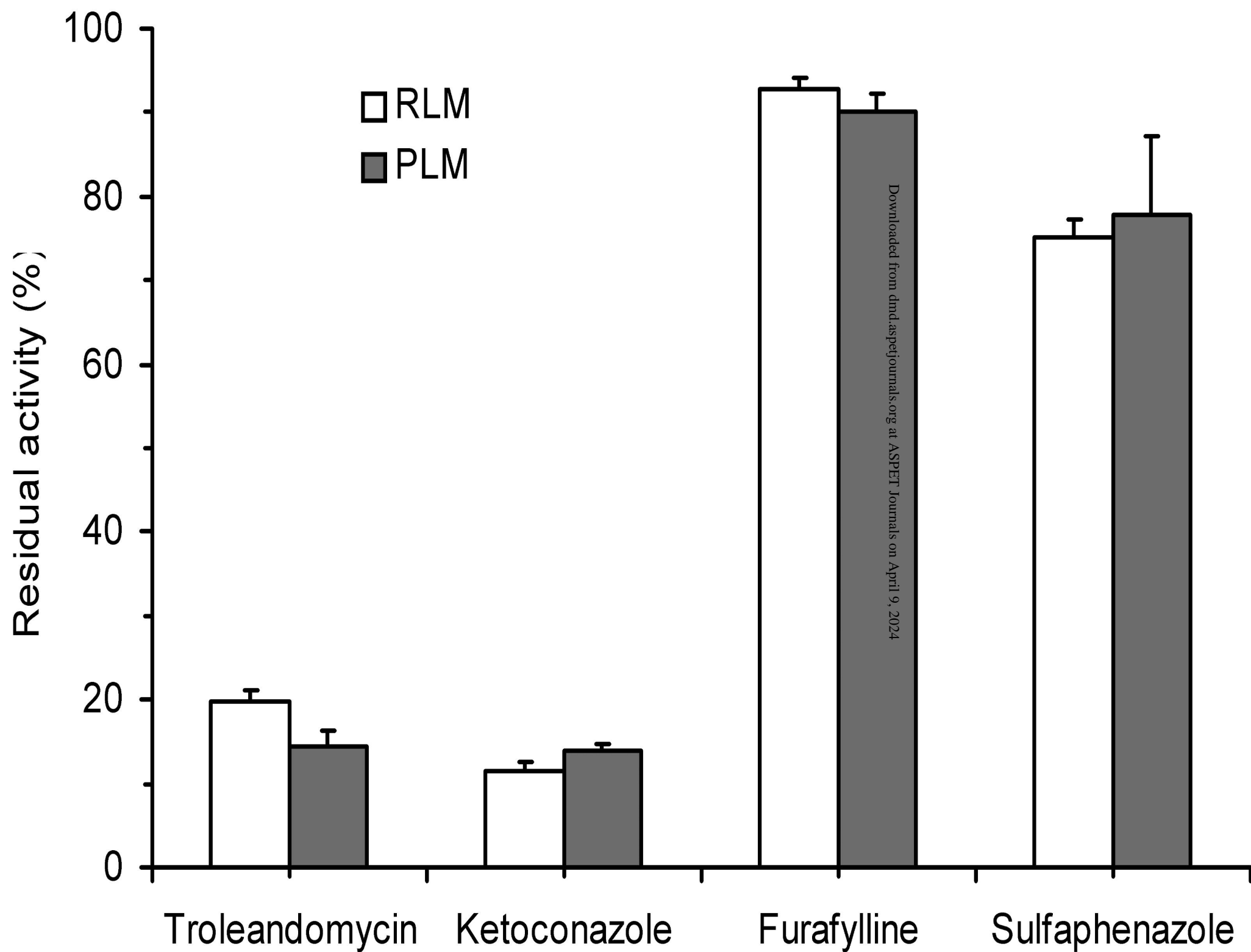


Fig.6

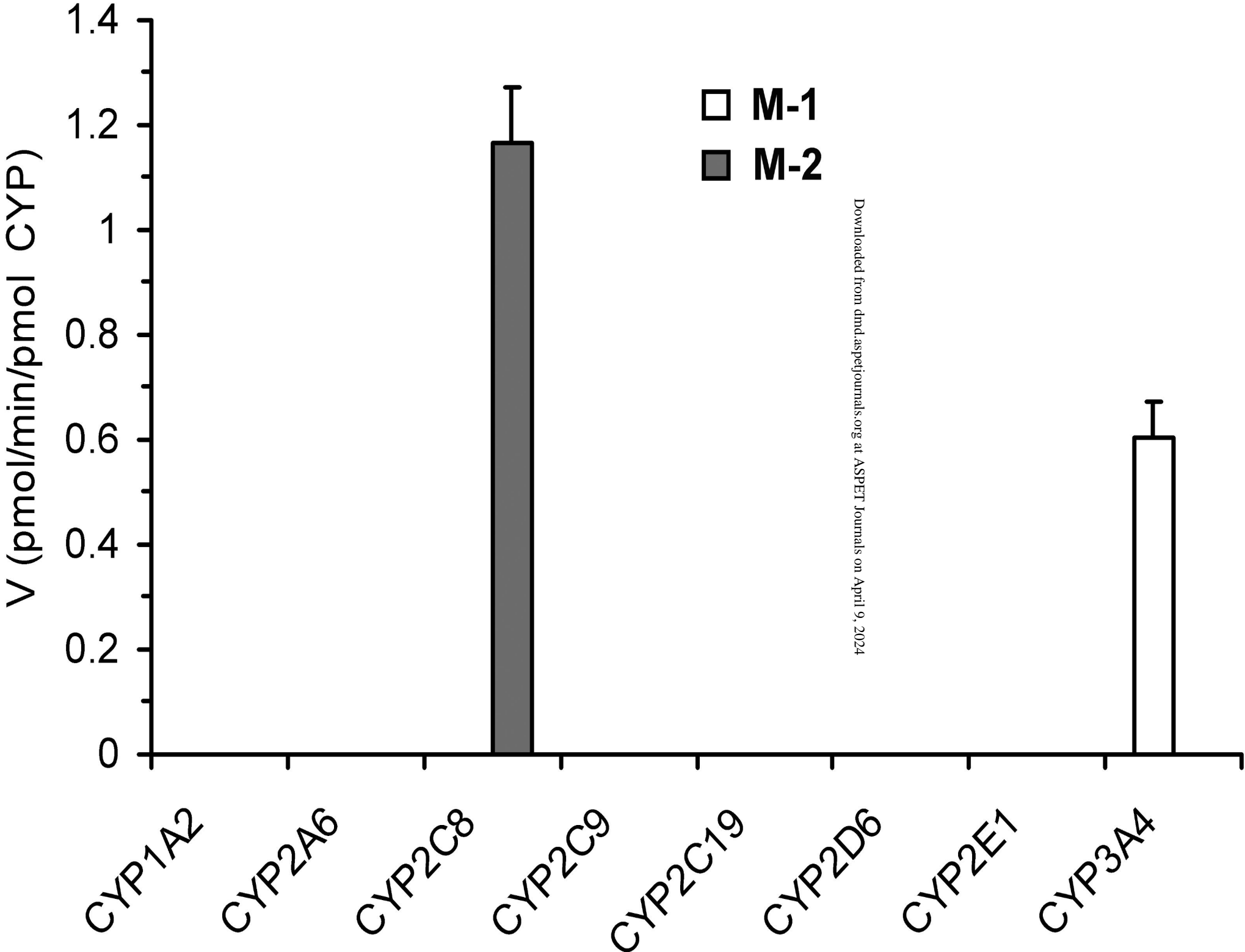


Fig.7

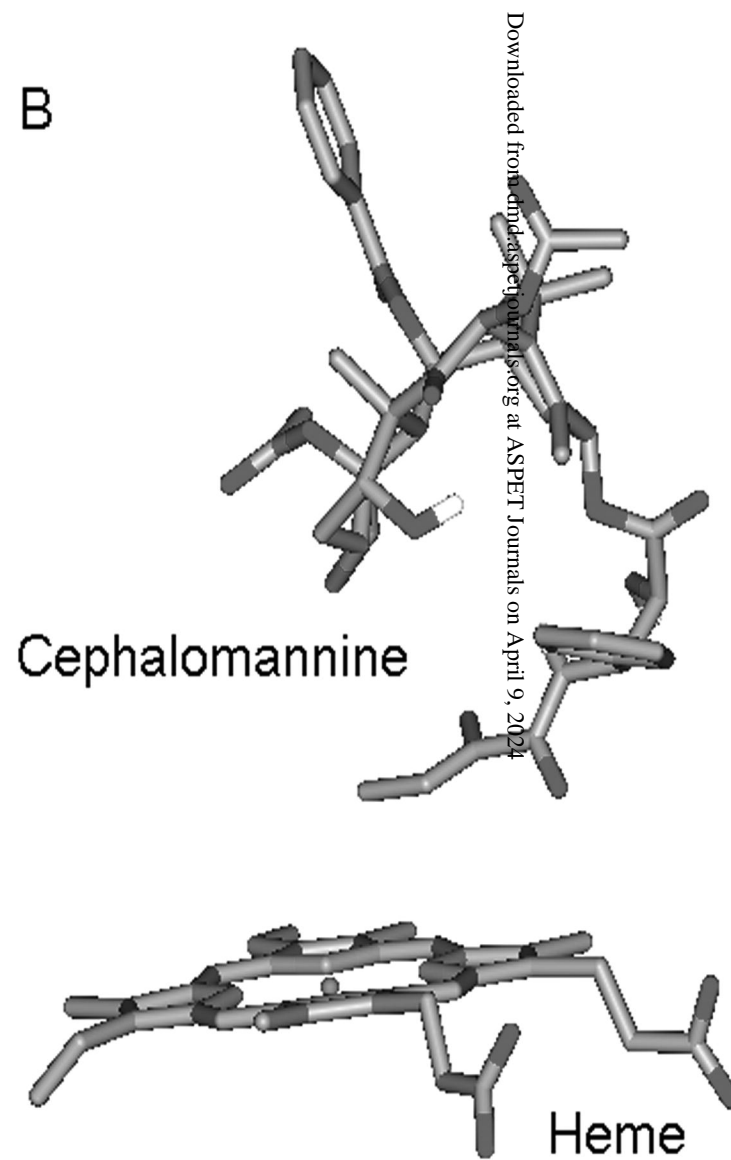
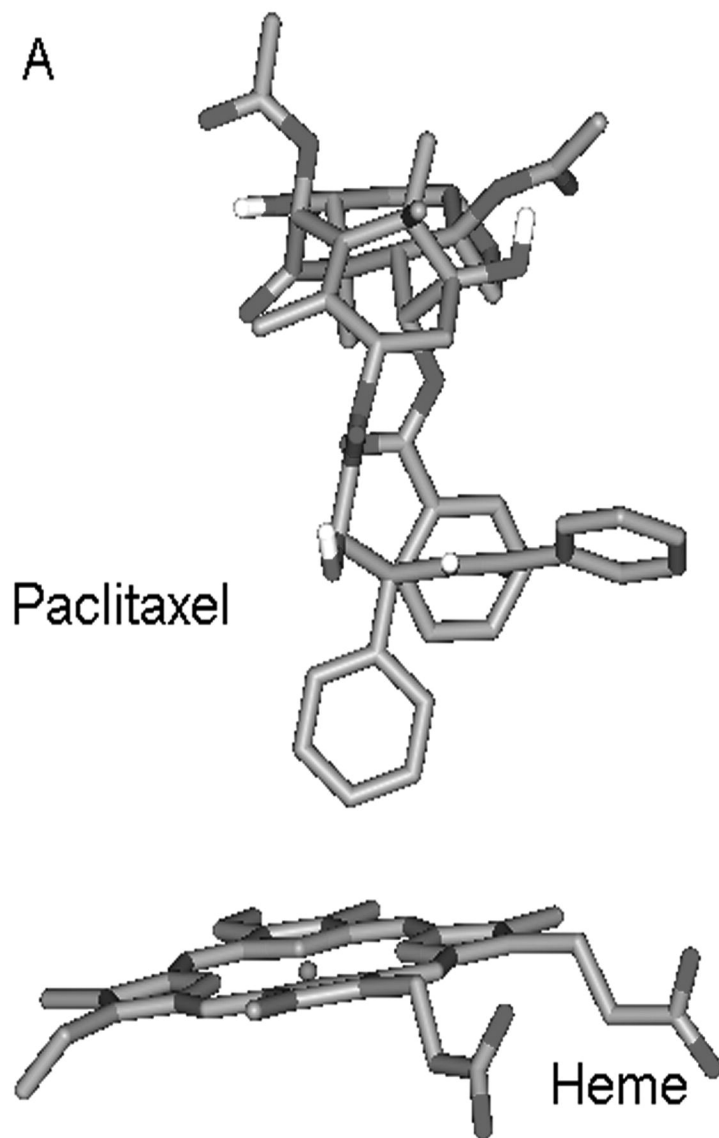


Fig.8

